Sensors and Actuators A 161 (2010) 114–119

Contents lists available at ScienceDirect

Sensors and Actuators A: Physical

journal homepage: www.elsevier.com/locate/sna

Analysis of small deflection touch mode behavior in capacitive pressure sensors

Giulio Fragiacomo[a,*], Thor Ansbæk[b], Thomas Pedersen[a], Ole Hansen[a,c], Erik V. Thomsen[a]

[a] Department of Micro- and Nanotechnology, Technical University of Denmark, DTU Nanotech, Building 345E, DK-2800 Kgs. Lyngby, Denmark
[b] Department of Photonics Engineering, Technical University of Denmark, DTU Fotonik, Building 343, DK-2800 Kgs. Lyngby, Denmark
[c] Centre for Individual Nanoparticle Functionality, Technical University of Denmark, Building 345E, DK-2800 Kgs. Lyngby, Denmark

ARTICLE INFO

Article history:
Received 23 October 2009
Received in revised form 4 March 2010
Accepted 12 April 2010
Available online 10 May 2010

Keywords:
Plate deflection
Analytical model
Capacitive sensor
Touch mode

ABSTRACT

Due to an increasing need for devices with low power consumption, capacitive pressure sensors have become good substitutes for the well known piezoresistive pressure sensors. Mathematical models are necessary to design and characterize the device, preferably the model is analytical such that geometrical scalings are revealed. We show that, in the case of linear elastic behavior, a simple analytical model can be found for a touch mode capacitive pressure sensor (TMCPS). With this model it is possible to readily evaluate the main features of a TMCPS such as: sensitivity (both in normal and touch mode), touch point pressure and parasitic capacitance. Therefore, the desired device can be designed without using finite element modeling (FEM). This reduces the effort needed to design a micromachined TMCPS. Finally, the model has been compared with a micromachined TMCPS showing an excellent agreement with the experimental data.

1. Introduction

Micromachined pressure sensors, both capacitive and piezoresistive, have been among the most successful MEMS (Micro Electro-Mechanical Systems) developed in the last 40 years [1,2].

Capacitive pressure sensors typically consist of a plate and a substrate, both conductive, separated by insulating media (e.g. silicon dioxide and air as shown in Fig. 1) [3]. The capacitance of the device increases when pressure is applied on the plate causing its deflection toward the substrate. These sensors can be designed to work in normal mode, where the deflection of the plate is smaller than the cavity height, or in touch mode when the plate touches the insulator on the bottom electrode. Here we present a simple analytical model for touch mode capacitive pressure sensors. Depending on the ratio between the height of the cavity (or gap distance) and the plate thickness, this type of sensors will work in a linear elastic regime or in a large deflection regime. We only treat the case of linear elastic deformations of a circular isotropic plate, i.e. the gap distance is less than half of the plate thickness [4,5].

Previous work on mathematical models for capacitive pressure sensors have been presented [6–9]. The problem has been approached with different techniques, such as assuming a power series solution [6–8] and using the pseudo spectral method [9], where in both cases the principle of virtual work is used to find the displacement for large deflection. In this work, we will show that a closed form expression exist for touch mode capacitive pressure sensors (TMCPSs) in the linear elastic regime, or that is for small deflections. We will also show how it is possible to obtain a fitting function describing the relationship between capacitance and pressure for microfabricated TMCPS from this model. To validate our model we will apply it to a microfabricated TMCPS, the fabrication of which is described elsewhere [10,11]. In the following discussion three main topics will be covered, firstly, in Section 2, a general theory that can be used to model TMCPS will be presented, then, in Section 3, a description of the sensor fabricated will be provided and finally, in Sections 4 and 5, the measurement setup and a comparison between the model and the experimental results will be presented.

2. Theory

The capacitance–pressure curve (C–P) describing the behavior of a micromachined TMCPS can be divided into three different zones of interest: normal, transition and touch mode [12]. The region before the top plate reaches the bottom of the cavity is referred as the normal mode operation. Around the point where the plate touches the bottom of the cavity there is a highly nonlinear relationship between capacitance and pressure where the sensor is said to be in the transition zone. Finally, when the membrane is in contact with the insulator layer, which is placed on the bottom of the cavity to avoid short circuit of the device, the sensor works in touch mode.

* Corresponding author at: Ørsted plads, bygning 345, Room 118, 2800 Copenhagen, Denmark. Tel.: +45 256316.
E-mail addresses: giulio.fragiacomo@nanotech.dtu.dk, gifr@nanotech.dtu.dk (G. Fragiacomo).

0924-4247/$ – see front matter © 2010 Elsevier B.V. All rights reserved.
doi:10.1016/j.sna.2010.04.030

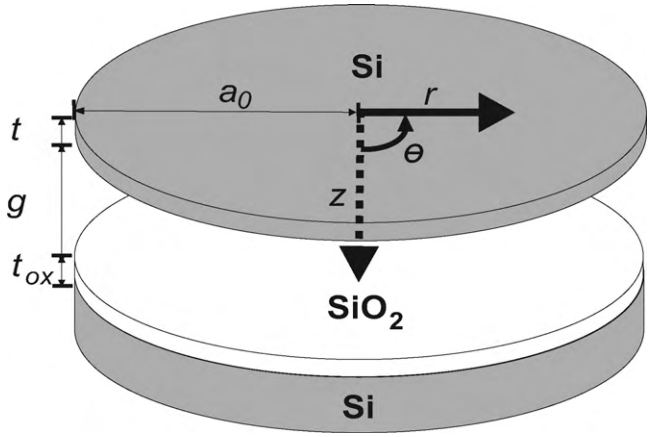

Fig. 1. Schematic of the capacitive element. Both upper and lower plates are made of heavily doped silicon while the insulator layer is made of silicon dioxide. The polar coordinates used in this work are shown as well as some of the main dimensions such as the plate thickness t, the oxide thickness t_{ox}, the radius a_0 and the gap distance g.

In this section we will show that, for circular clamped plates, under the linear elastic approximation, it is possible to obtain a reliable model just by dividing the problem into two: normal mode and touch mode. In the following sections this model will be used to derive the main design parameters of a microfabricated TMCPS.

2.1. Normal mode

Here the diaphragm type under consideration is that of a uniformly loaded circular plate with radius a_0 and thickness t, see Fig. 1. The mechanical properties of the plate are characterized by the isotropic Young's modulus E and the Poisson ratio ν. The differential equation, also called governing equation, describing the displacement as a function of the radial coordinate, $w(r)$, under pure bending can be written in terms of the applied external pressure, p, as [4]

$$D\nabla^2\nabla^2 w = p, \tag{1}$$

where D is the flexural rigidity of the plate given by

$$D = \frac{Et^3}{12(1-\nu^2)}. \tag{2}$$

To simplify determination of the constants of integration in a solution to Eq. (1) it is useful to calculate the shearing force per unit length F in the plate; F can be calculated from the force balance equation

$$2\pi rF = \int 2\pi pr\ dr, \tag{3}$$

where r is the radial position, therefore

$$F(r) = \frac{pr}{2} + \frac{c}{r}, \tag{4}$$

where c is a constant of integration. In the normal mode case c is trivially zero as can also easily be seen if a definite integral had been used in Eq. (3); however, in the touch mode case which we shall consider later $c \neq 0$ and then Eq. (4) is needed for identification of c. Thus the deflection of a circular diaphragm fixed at the perimeter can be obtained solving Eq. (1) [4]

$$w(r,p) = \frac{pa_0^4}{64D}\left(1-\left(\frac{r}{a_0}\right)^2\right)^2 \equiv w_0\left(1-\left(\frac{r}{a_0}\right)^2\right)^2, \tag{5}$$

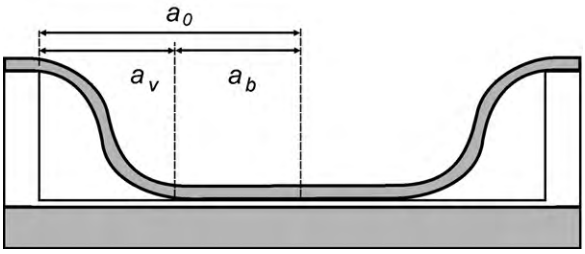

Fig. 2. Touch mode operation. When the sensor is working in touch mode the problem is split into two parts: the touching circular area of radius a_b and the untouched area which is an annular region of inner radius a_b and outer radius a_0; a_v is defined as the difference between the outer and the inner radii.

where w_0 is referred to as the center deflection and is a function of the pressure p. From Eq. (5) the capacitance can be found as

$$C = \int_0^{2\pi}\int_0^{a_0} \frac{\epsilon_0\epsilon_{ox} r\, dr\, d\theta}{t_{ox} + \epsilon_{ox}(g - w(r))} = C_0 \frac{\arctan h(\sqrt{\xi})}{\sqrt{\xi}}, \tag{6}$$

where ξ is the ratio of the center deflection to the effective thickness of the dielectric

$$\xi \equiv \frac{w_0}{g((t_{ox}/g\epsilon_{ox}) + 1)}, \tag{7}$$

and

$$C_0 \equiv \frac{\pi\epsilon_0\epsilon_{ox}a_0^2}{g\epsilon_{ox} + t_{ox}}, \tag{8}$$

is the parallel plate capacitance for a vacuum–gap distance of g and a thin insulation layer of oxide on the bottom plate of thickness t_{ox} and relative dielectric constant ϵ_{ox}.

2.2. Touch mode

When the top diaphragm of the capacitor comes into contact with the fixed bottom plate a transition occurs to a different operation mode, referred to as touch mode (see Fig. 2). In this case, the center point of the plate is no longer a part of the solution of Eq. (1) and the shearing force must vanish at the touching line so the constant of integration of Eq. (4) assumes the following value

$$c = -\frac{1}{2}a_b^2 p, \tag{9}$$

where a_b is the radius of the touching surface. With this assumption, the governing equation has been solved [4] but, even neglecting the stretching effect in the plate, the expression obtained is not suitable for the evaluation of the capacitance as a function of the applied load done later on in this section. A simpler approach considers the total capacitance as being made up by two distinct parts [7,8]. One is given by the part of the diaphragm where the two electrodes are separated by the insulating oxide. This part is a simple parallel plate capacitor with a fixed oxide gap of t_{ox} and a radius a_b that increases with an increasing pressure. The second is given by the annular part of the diaphragm which is not touching the bottom electrode and has a fixed outer radius a_0 but a varying inner radius a_b which increases with increasing pressure, thus decreasing the area not touching the bottom electrode (the total area subtracted the area touching the bottom electrode). Therefore, we will assume that the deflection function in touch mode can be approximated by

$$w(r,p) = \begin{cases} g & 0 < r < a_b(p) \\ g\left(1-\left(\dfrac{r-a_b(p)}{a_v(p)}\right)^2\right)^2 & a_b(p) < r < a_0 \end{cases}, \tag{10}$$

where the radius of the plate touching the bottom of the cavity, a_b, is a function of pressure as is also the part of the diaphragm not

touching the bottom plate, a_v. Furthermore, Eq. (10), which will be used to model the shape of the deflected plate, is seen to satisfy the boundary conditions

$$w(a_0)=0,\quad \frac{dw}{dr}|_{r=a_0}=0,\quad w(a_b(p))=g,\quad \frac{dw}{dr}|_{r=a_b(p)}=0. \tag{11}$$

Note that $a_0-a_b=a_v$, thus there is only one independent variable. Inspired by the work of [7,8], we calculate the variable a_v by considering only the part of the plate bending, excluding the part touching the bottom of the cavity. In the simplified model proposed, the center point deflection is forced to equal the gap distance $w(0, p)=w_0=g$. If the membrane only touches in the center point $a_v=a_0$, and the pressure is obtained from Eq. (5). We now assume that Eq. (5) remains valid at higher pressures if a_0 is replaced by a_v and thus

$$a_v(p)\equiv\left(\frac{64Dg}{p}\right)^{1/4}. \tag{12}$$

In other words the radial deflection profile of the part of the diaphragm not touching the bottom electrode is taken to be the same as that of the diaphragm in normal mode. This will be shown, in Section 5, to be a reasonable assumption as has been shown for the case of large deflection [7,8]. The capacitance in touch mode using Eq. (10) is found to have an analytical expression

$$\begin{aligned}C&=\int_0^{2\pi}\int_0^{a_0}\frac{\epsilon_0\epsilon_{ox}r\,dr\,d\theta}{t_{ox}+\epsilon_{ox}(g-w(r))}\\&=\frac{\epsilon_0\epsilon_{ox}\pi a_b^2}{t_{ox}}+\frac{2\pi\epsilon_0\epsilon_{ox}}{g\epsilon_{ox}+t_{ox}}\int_{a_b}^{a_0}\frac{r}{1-\gamma(1-((r-a_b)/a_v)^2)^2}dr,\end{aligned} \tag{13}$$

where

$$\gamma\equiv\frac{1}{(t_{ox}/g\epsilon_{ox})+1}, \tag{14}$$

is a constant related to sensor design and attains a value between zero and one, $\gamma\in]0;1[$. For a large gap distance compared to the oxide thickness, γ will be close to 1. This is an interesting case which is considered in the following section since such a design has the largest sensitivity. Introducing a change of variables $u\equiv(r-a_b)/a_v$, the integral χ of Eq. (13) can be further simplified

$$\begin{aligned}\chi&=\int_{a_b}^{a_0}\frac{r}{1-\gamma(1-((r-a_b)/a_v)^2)^2}dr\\&=a_v^2\int_0^1\frac{u}{1-\gamma(1-u^2)^2}du+a_ba_v\int_0^1\frac{1}{1-\gamma(1-u^2)^2}du\end{aligned} \tag{15}$$

$$\equiv(k_1a_v^2+k_2a_ba_v), \tag{16}$$

where the two integrals k_1 and k_2, are independent of the pressure. These two integrals can be solved analytically as follows:

$$k_1=\frac{1}{2}\frac{\arctan h\sqrt{\gamma}}{\sqrt{\gamma}} \tag{17}$$

$$k_2=\frac{\arctan\left((\sqrt{\gamma})/\left(\sqrt{\sqrt{\gamma}-\gamma}\right)\right)}{2\sqrt{\sqrt{\gamma}-\gamma}}+\frac{\arctan h\left((\sqrt{\gamma})/\left(\sqrt{\sqrt{\gamma}+\gamma}\right)\right)}{2\sqrt{\sqrt{\gamma}+\gamma}}, \tag{18}$$

both k_1 and k_2 vary from 0 to ∞ as γ varies from 0 to 1.

Inserting Eq. (16) in Eq. (13) and rearranging in terms of the virtual radius a_v the capacitance in touch mode can be written as

$$C=C_{ox}\left(\left(1+2\frac{k_1-k_2}{\left((g\varepsilon_{ox}/t_{ox})+1\right)}\right)\frac{a_v^2}{a_0^2}+2\left(\frac{k_2}{\left((g\varepsilon_{ox}/t_{ox})+1\right)}-1\right)\frac{a_v}{a_0}+1\right), \tag{19}$$

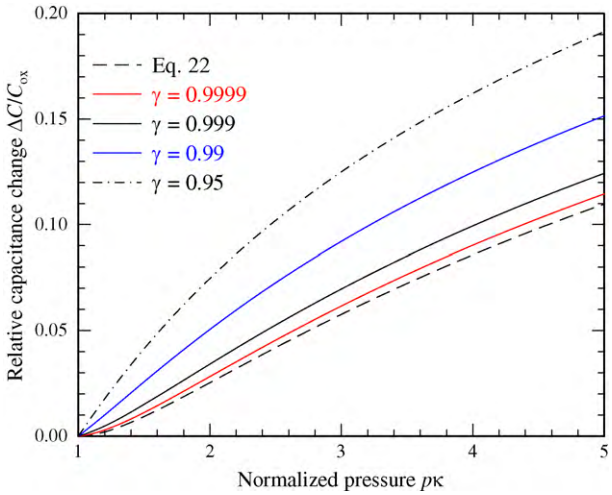

Fig. 3. Comparison between the touch mode capacitance, Eq. (19), as a function of normalized pressure κp calculated at different values of γ and the capacitance calculated from Eq. (22).

where C_{ox} is the oxide capacitance

$$C_{ox}\equiv\epsilon_0\epsilon_{ox}\frac{\pi a_0^2}{t_{ox}}. \tag{20}$$

Thus, the capacitance of a sensor in touch mode can be described as a second order polynomial in terms of a_v which is linked, as shown in Eq. (12), to the applied pressure.

2.2.1. Special case $g\epsilon_{ox}\gg t_{ox}$

The special case, where the product of the gap distance and the dielectric constant of the oxide is much larger than the oxide thickness, is interesting from a device design point of view, when high sensitivity is desired. Using this assumption in Eq. (19) together with Eq. (12) and defining

$$\kappa=\frac{a_0^4}{64Dg}, \tag{21}$$

the capacitance becomes

$$C\approx C_{ox}\left(\sqrt{\frac{1}{\kappa p}}-2\sqrt[4]{\frac{1}{\kappa p}}+1\right), \tag{22}$$

and it is seen that C is a polynomial in $(\kappa p)^{-1/4}$. Note, that also the capacitance of Eq. (19) is a second order polynomium in $(\kappa p)^{-1/4}$, the coefficients though are different and are functions of γ only. This makes it simple to fit the capacitance–pressure curve in touch mode, as it can be seen in Section 4. Even though the results obtained will show that, in our case, this approximation gives a simple and reliable way to estimate the characteristics of the device fabricated, it should be kept in mind that it is based on the fact that the two terms $(k_1-k_2)/\left((g\varepsilon_{ox}/t_{ox})+1\right)$ and $k_2/((g\varepsilon_{ox}/t_{ox})+1)$, in Eq. (19), were taken to be negligible and that will intrinsically affect the accuracy of this model. For the sensor fabricated, $\gamma=0.982$ and these two terms are −0.127 and 0.151, respectively.

In Fig. 3 the relative capacitance change $\Delta C/C_{ox}$ from Eq. (19) is plotted as a function of normalized pressure κp at different values of γ; for comparison also Eq. (22) is shown and it is seen that as γ approach 1 the two expressions agree.

3. Sensor design

A micromachined TMCPS previously fabricated, see [10,11], was used in order to validate the model presented in Section 2. It consist of an array of hexagonal clamped silicon plates suspended by

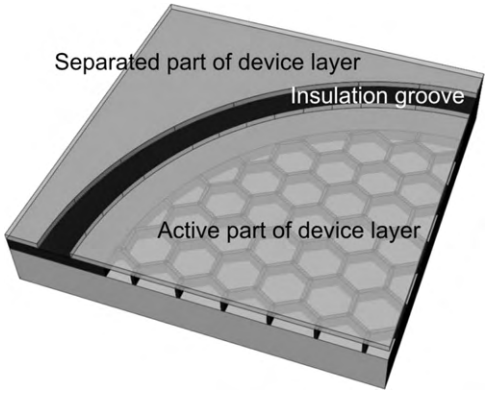

Fig. 4. Artists view of the micromachined TMCPS. The active area of the sensor is given by N silicon plates with hexagonal shape. The capacitors given by each single element are in parallel. An insulating groove separates the active area from the rest of the device in order to reduce parasitic capacitance.

a SiO_2 honeycomb structure (see Fig. 4). The capacitors are therefore made up by a three layer structure: two heavily doped silicon layers with a thin silicon dioxide layer in between. Furthermore, to enhance temperature insensitivity, the cavities are sealed in vacuum (10^{-2} mbar nitrogen) using a fusion bonding technique [14]. This design is implemented to minimize problems arising from parasitic capacitance, often one of the major issues for capacitive sensors [15]. A parallel combination of capacitors is then obtained, therefore the overall sensor capacitance is given by [10]:

$$C(p) = NC_c(p) + C_p, \tag{23}$$

where N is the number of plates (in this case $N = 180$), C_c is the capacitance due to the active area and C_p is the parasitic capacitance. The clamped plates of the TMCPS consist of the device layer of a SOI wafer and part of its buried oxide. The plate thickness has a nominal value of $t = 2.5 \pm 0.7\ \mu m$ with $2 \pm 0.5\ \mu m$ of Si and $0.5 \pm 0.2\ \mu m$ of SiO_2. On a silicon wafer, that is fusion bonded to the SOI wafer, a thermally grown oxide defines the gap distance which is $g = 420 \pm 5$ nm. Since the gap distance is much smaller than half of the plate thickness, this kind of sensor will work in the linear elastic regime. It is important to point out that this is the only requirement in the model presented in the previous section. Any circular clamped plate that fulfill this requirement can be described by the analytical model presented.

In order to calculate a fitting function for the C–P curve of this sensor another important parameter is needed: the radius of the plate which has been approximated with the inner radius of the hexagons $a_0 = 75 \pm 1\ \mu m$. During fabrication it is also possible to measure the thickness of the insulator layer on the bottom of the cavity which results in approximately $t_{ox} = 30 \pm 5$ nm. Finally, from the geometrical and material properties of the sensor described, it is possible to estimate all the parameters of interest such as the parallel plate capacitance, C_0, the parasitic capacitance, C_p, the flexural rigidity, D and the touch point pressure p_t. All these values are reported in Table 1.

Table 1
Calculated parameters of the sensor fabricated.

Parameter	Calculated value
NC_0	66.0 pF
C_p	61 pF
D	2.0×10^{-7} N m
p_t	1.70 bar

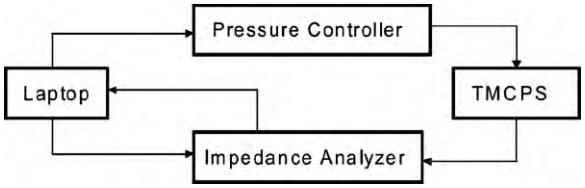

Fig. 5. Schematic of the measurement setup. A Druck DPI 520 pressure controller and a HP 4294A Precision Impedance Analyzer are controlled by a laptop where a Labview code has been implemented. For each pressure value applied on the TMCPS an impedance measurement is performed by the analyzer.

Table 2
Measured geometrical values of the sensor fabricated.

Parameter	Measured value
a_0	$75\ \mu m \pm 1\ \mu m$
N	180
g	$420\ nm \pm 5\ nm$
t_{ox}	$30\ nm \pm 5\ nm$

4. Measurement setup

The TMCPS described in the previous section has been characterized with a measurement setup consisting of a Druck DPI 520 pressure controller and a HP 4294A Precision Impedance Analyzer (see Fig. 5). Both instruments have been connected to a laptop and controlled by a custom Labview program. The C–P curve has been obtained varying the pressure from 250 mbar to 10.9 bar in steps of 26 mbar.

5. Fitting

In this section a fit to the measured C–P data, using Eqs. (6) and (22), is done. Using the measured values presented in Table 2, fitting parameters are calculated and physical quantities such as the flexural rigidity and the parasitic capacitance are estimated.

5.1. Normal mode

Fig. 6 shows the capacitance pressure characteristics for the sensor when working in normal mode. Eq. (6) is a useful starting point for analysis of the sensor. By adding a parasitic capacitance C_p and

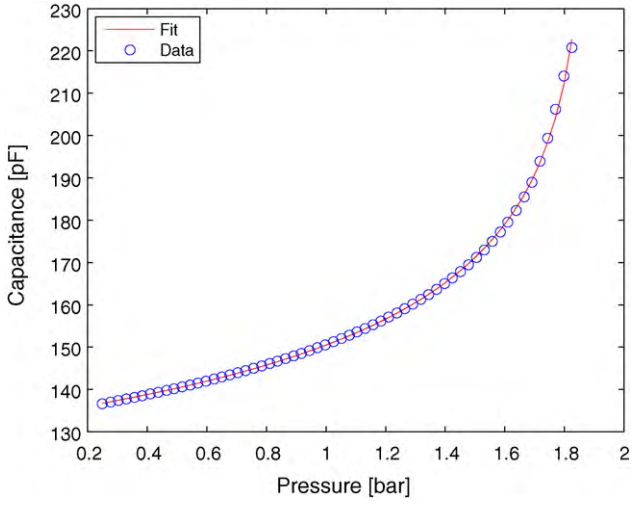

Fig. 6. Capacitance pressure characteristics of the sensor in normal mode. The solid line represent the fit calculated using Eq. (26), on the data points (circles) measured from 250 mbar to 1.8 bar.

Table 3
Results from the analysis of normal mode behavior.

Parameter	Fitted value
NC_0	62.0 pF
C_p	71.8 pF
D	2.19×10^{-7} N m

assuming $g\epsilon_{ox} \gg t_{ox}$, we obtain

$$\xi = \frac{w_0}{g((t_{ox}/g\epsilon_{ox})+1)} \approx \frac{w_0}{g}, \tag{24}$$

and

$$C(p) = NC_c(p) + C_p = NC_0\sqrt{\frac{1}{\kappa p}}\arctan\mathrm{h}\left(\sqrt{\kappa p}\right) + C_p, \tag{25}$$

Noting, that $C(0) = NC_0 + C_p$, we can write

$$C = NC_0\left(\sqrt{\frac{1}{\kappa p}}\arctan\mathrm{h}\sqrt{\kappa p} - 1\right) + C(0), \tag{26}$$

which is a suitable fitting function with three parameters C_0, $C(0)$ and κ to be determined from the plot. This expression has been used as a fitting function to analyze the data shown in Fig. 6, the solid line shows the fit. As a_0, N and g can be measured it is possible to obtain the effective plate stiffness, D, from the fit. The extracted values are shown in Table 3. The rigidity is as expected around 2×10^{-7} N m, as can be estimated from Eq. (2).

5.2. Touch mode

In Fig. 7 the overall capacitance pressure characteristics is shown. The fact that Eq. (19) can be represented by a second order polynomium in $p^{-1/4}$ is used in this section for analysis of the sensor when working in touch mode (see Fig. 2). By adding a parasitic capacitance, C_p, to Eq. (19) we obtain

$$C(p) \equiv b_0 + b_1 p^{-1/4} + b_2 (p^{-1/4})^2, \tag{27}$$

where the coefficients are $b_0 = NC_{ox} + C_p$, $b_1 = -2[1 - k_2(1-\gamma)]NC_{ox}/\sqrt[4]{\kappa}$, and $b_2 = [1 + 2(1-\gamma)(k_1 - k_2)]\,NC_{ox}/\sqrt{\kappa}$.

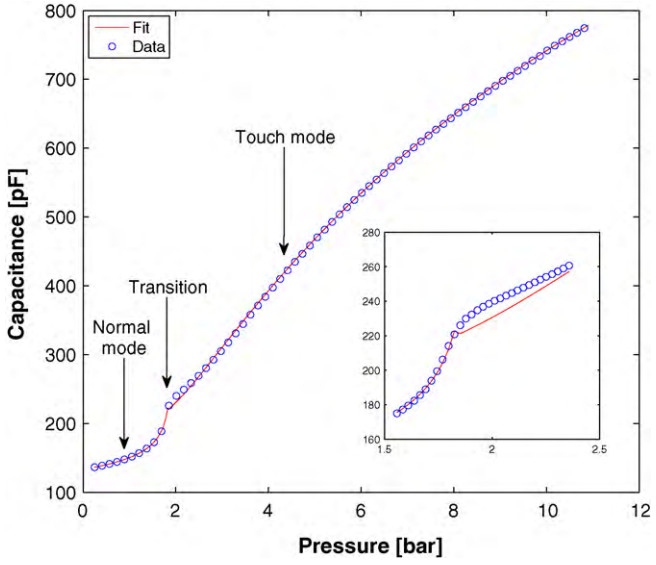

Fig. 7. Capacitance pressure characteristics in normal, transition and touch mode. Using Eqs. (26) and (27) a curve (solid line) that can fit the data points (circles) measured both in normal and touch mode has been obtained.

Table 4
Results from the analysis of touch mode behavior.

Parameter	Fitted value
t_{ox}	27.5 nm
C_p	70.5 pF
D	2.72×10^{-7} N m

From the relation between γ and the capacitance ratio

$$\gamma = 1 - \frac{NC_0}{NC_{ox}} = 1 - \frac{NC_0}{b_0 - C_p}, \tag{28}$$

we calculate γ, which is very insensitive to errors in the parasitic capacitance C_p since $NC_{ox} \gg C_p$ (for the present sensor C_p is less than 2% of NC_{ox}). The oxide thickness may be calculated directly from

$$t_{ox} = N\frac{\pi a_0^2 \epsilon_0 \epsilon_{ox}}{NC_{ox}} = N\frac{\pi a_0^2 \epsilon_0 \epsilon_{ox}}{b_0 - C_p}, \tag{29}$$

which also is quite insensitive to C_p. Finally, the flexural rigidity (and thus κ) may be calculated from

$$D = \frac{1}{4g}\left(\frac{a_0 b_2}{-b_1}\right)^4 \frac{[1 - k_2(1-\gamma)]^4}{[1 + 2(1-\gamma)(k_1 - k_2)]^4}, \tag{30}$$

while the exact value of C_p is calculated such that the coefficients b_0, b_1, and b_2 are consistent with the calculated parameters.

Thus, the oxide thickness t_{ox}, the parasitic capacitance C_p and the flexural rigidity D can be obtained from the fit. Table 4 shows the extracted values in the touch mode case. The oxide thickness is in good agreement with the fabrication value and the value extracted for the parasitic capacitance is close to the one reported in Table 3 for the normal mode case. Also here, the rigidity is around 2×10^{-7} N m.

In the next section we will use the results obtained from this section in order to fit the entire C–P curve of the TMCPS described previously.

6. Discussion

In the previous section the problem was split into two: the normal mode and the touch mode region. Combining Eqs. (26) and (27) it is possible to obtain a fitting function for the entire C–P curve as it is shown in Fig. 7. An excellent match between the data points and the fitting functions is obtained both in the normal mode and in the touch mode region. As shown in the inset of Fig. 7, the model does not give as satisfactory as result in the transition region because pull in and adhesive forces have not been taken into account. None the less, the maximum deviation of the model from the data points is only 3.7%. Comparing the extracted values of Tables 3 and 4, two different results for the flexural rigidity are found. This is due to the fact that when the plate touches the bottom of the cavity it becomes stiffer as was noticed in previous work [13]. So, in order to obtain an accurate result for this parameter, both stretching effects and the exact value of the terms in Eq. (19) should be taken into account in the fitting function. As seen from Table 4 the fit allows extraction from measurements of the parasitic and ideal capacitance value, the latter being within 10% of the value calculated from the geometrical parameters. The parasitic capacitance extracted from the measurements $C_p \sim 72$ pF is larger than the calculated value of 61 pF, since the calculated parasitic is the pure die parasitic capacitance. The bonding wires, the chip carrier and the measurement setup add some capacitance that may explain the discrepancy; for instance we have measured 4 pF for an empty chip carrier.

The touch point pressure has been estimated to be at the maximum in the sensitivity curve which is given by the first derivative of the C–P curve, this can easily be extracted from the data points collected. The experimental result of 1.77 bar compares well to the

expected value of 1.70 bar as estimated in Table 1. Furthermore, by using this model, the sensor can be designed to work in a specific range of pressures without entering in the saturation region where the capacitance is constant even if the pressure applied increases. Finally we would like to point out what can be achieved from a design perspective; under the hypothesis of linear elastic regime, given a set of fixed parameters such as the plate radius, the plate thickness and the oxide thickness it is easy to evaluate important design parameters such as the capacitance and the sensitivity of the device. Therefore it is possible to use this model to predict the desired *C–P* curve and to evaluate the parasitic capacitance of the sensor when fabricated.

7. Conclusions

An analytical model for TMCPS has been presented. It has been shown that, in the linear elastic regime, there is a closed form solution to the integral defining the capacitance of a device driven into touch mode. Combining this with the solution found for a device working in normal mode a fitting function for the entire *C–P* curve has been found.

The fitting function has been tested using a device working in the linear elastic regime and an excellent match between fitted and measured parameters has been shown. With the derived analytical model a TMCPS can be designed to have the desired capacitance and sensitivity by fixing a set of fabrication parameters.

References

[1] M. Gad-El-Hak, The MEMS Handbook, CRCnetBASE Product, 2002.
[2] L.K. Baxter, Capacitive Sensors: Design and Applications, 1st ed., IEEE Press, 1997.
[3] A.V. Chavan, K.D. Wise, A batch-processed vacuum-sealed capacitive pressure sensor, in: IEEE Transducers, 1997, pp. 1449–1452.
[4] S.P. Timoshenko, S. Woinkowsky-Krieger, Theory of Plates and Shells, 2nd ed., McGraw-Hill, New York, 1959.
[5] R. Szilard, Theories and Applications of Plate Analysis, 1st ed., Wiley, 2004.
[6] W.H. Ko, Q. Wang, Touch mode capacitive pressure sensor, Sensors and Actuators 75 (1999) 242–251.
[7] G. Meng, W.H. Ko, Modeling of circular diaphragm and spreadsheet solution programming for touch mode capacitive sensors, Sensors and Actuators 75 (1999) 45–52.
[8] M. Daigle, J. Corcos, K. Wu, An analytical solution to circular touch mode capacitor, IEEE Sensors Journal 7 (2007) 502–505.
[9] X. Wang, L. Mingxuan, C. Wang, Numerical analysis of capacitive pressure micro-sensors, Science in China Series E: Engineering & Materials Science 48 (2005) 202–213.
[10] T. Pedersen, O. Hansen, E.V. Thomsen, Reduction of hysteresis in capacitive pressure sensors, in: Proceedings of EUROSENSOR XXII, 2008, pp. 165–168.
[11] T. Pedersen, G. Fragiacomo, O. Hansen, E.V. Thomsen, Highly sensitive micromachined capacitive pressure sensor with reduced hysteresis and low parasitic capacitance, Sensors and Actuators A 154 (2009) 35–41.
[12] W.H. Ko, Q. Wang, Modeling of touch mode capacitive sensors and diaphragms, Sensors and Actuators 75 (1999) 230–241.
[13] W.H. Ko, Q. Wang, Touch mode capacitive pressure sensors for industrial applications, in: Proceedings IEEE The Tenth Annual International Workshop on Micro Electro Mechanical Systems, 1997, pp. 284–289.
[14] A. Bertold, Low Temperature Wafer-to-wafer Bonding for Micromachined Systems, 1st ed., Deltech Uitgevers, 2001.
[15] B. Puers, E. Peters, A.V. den Bossche, W. Sansen, A capacitive pressure sensor with low impedance output and active suppression of parasitic effects, Sensors and Actuators 21 (1990) 108–114.

Biographies

Giulio Fragiacomo received his MSc degree in electronics engineering in 2008 from Università degli Studi di Trieste and is currently employed as PhD student in physics and nanotechnology at the Technical University of Denmark. He has been working on micromachined capacitive pressure sensors since the beginning of 2008. His project has been supported by Grundfos A/S. His interests are MEMS devices, analog electronics and solid-state electronics.

Thor Ansbæk received his MSc degree in 2008 from The Technical University of Denmark, Department of Micro and Nanotechnology. He has been working with the development and fabrication of a telemetric capacitive pressure sensor. Currently, he is employed as PhD student at DTU Fotonik where he is working in the area of micro-electromechanical systems and vertical-cavity surface-emitting laser diodes for medical diagnosis. He is a board member of the Electrical Engineering Society of Denmark.

Thomas Pedersen received his MSc degree in 2006 from Technical University of Denmark, Department of Micro and Nanotechnology. He has been working with development and fabrication and of capacitive pressure sensors from 2005 to 2007 and is currently employed as a PhD student at DTU Nanotech. Currently, he is working with Piezoelectric Micromachined Ultrasound Transducers based on integration of MEMS technology and screenprinting of piezoelectric ceramic materials.

Ole Hansen received the MSc degree from the Semiconductor Laboratory, DTU, in 1977. Since then he has done research in silicon-based micro and nanotechnology and its applications, first at the Semiconductor Laboratory, and later at the Department of Micro and Nanotechnology, DTU Nanotech. Current research interests include deep reactive ion etching of silicon, $Si_{1-x}Ge_x$/Si heterostructures, microreactors for catalysis, and cantilever-based microprobes for nano-science. He is presently teaching three lecture courses: semiconductor technology, semiconductor devices and micro-electromechanical systems. Since 1990, he has been an associate professor at MIC, now DTU Nanotech. Since 2005 he has been part of the Danish National Research Foundation Center CINF, Center for Individual Nanoparticle Functionality.

Erik V. Thomsen is a group leader for the MEMS Applied Sensors activities at the MEMS section at the Department of Micro and Nanotechnology, Technical University of Denmark, DTU, where he is affiliated as professor. He holds a MSc in physics from Odense University and a PhD in electrical engineering from DTU. He has been affiliated with MIC, now DTU Nanotech, since 1992 and has been working with fabrication of semiconductor devices. His current interests include research and teaching within micromechanical multi-sensors, piezoresistivity of strained layers, piezoelectric MEMS devices, and micro-system packaging. He teaches classes in solid-state electronics, microtechnology and nano- and microfabrication.